HHS Public Access

Author manuscript

J Liposome Res. Author manuscript; available in PMC 2015 August 05.

Published in final edited form as:

J Liposome Res. 2015 June ; 25(2): 101–106. doi:10.3109/08982104.2014.932379.

^{99m}Tc-Labeled Porphyrin-Lipid Nanovesicles

Jae-Ho Lee[a,*], **Shuai Shao**[b], **Kenneth T. Cheng**[a], **Jonathan F. Lovell**[b], and **Chang H. Paik**[a]

[a]Radiopharmaceutical Laboratory, Division of Nuclear Medicine, Department of Radiology and Imaging Sciences, Warren G. Magnuson Clinical Center, National Institutes of Health, Bethesda, MD 20892, United States

[b]Department of Biomedical Engineering, University at Buffalo, State University of New York, Buffalo, NY 14260, United States

Abstract

Porphyrin-lipid nanovesicles (PLN) have been developed with intrinsic capabilities as activatable multimodal photonic contrast agents. Radiolabeling of PLN encapsulating drugs could eventually be able to provide quantitative *in vivo* information for diagnosing and treating diseases. In this study, we developed ^{99m}Tc-labeled porphyrin-lipid nanovesicles (^{99m}Tc-PLN) as a cargo-encapsulated formulation without significant impact on liposome integrity and encapsulation stability.50mM calcein was encapsulated into PLN by probe sonication. The size of the PLN was about 150nm. The PLN were then reacted with ^{99m}Tc using $SnCl_2$ dissolved in 1mMHCl as a reducing agent and incubated for 10 min at 22°C. The radiolabeling efficiency and stability of ^{99m}Tc-PLN were evaluated by instant thin-layer chromatography and low pressure liquid chromatography (LPLC). ^{99m}Tc labeling was successful with a >92% labeling efficiency. LPLC showed that the liposomal elution peaks of the porphyrin-lipid and the calcein overlapped with the radioactivity elution peak of ^{99m}Tc-labeled PLN. The ^{99m}Tc labeling procedure did not change the size of PLN. Encapsulated calcein remained inert inside PLN. Thus, this work lays out a simple and effective radiolabeling method using $SnCl_2$ in HCl for the preparation of ^{99m}Tc-PLN.

Keywords

Nanotechnology; Sustained release; ^{99m}Tc-labeled porphyrin-lipid nanovesicles; drug encapsulated liposome; size exclusion analysis

1. Introduction

Activatable drug release systems have attracted active research interests due to their possibility of maximizing drug efficacy and disease treatment, and improving imaging resolution by delivering drugs and imaging modalities agents in right times and places (Lee et al., 2013a, Snyder et al., 2003, Ellis et al., 2012, Goga et al., 2011, Guo et al., 2013). Activatable porphyrin-lipid nanovesicles (PLN) were developed based on porphyrin's innate

*Corresponding author: Tel.: +1 301 496 1426; fax: +1 301 402 4548., leejaeho@mail.nih.gov (Jae-Ho Lee, PhD).

Declaration of Interest

The authors report no declaration of interest.

properties that can be excited by 658nm laser and its fluorescent property (Lovell et al., 2011, Ng et al., 2013, Jin et al., 2013). When a 658nm laser excites porphyrin nanovesicles, porphyrin nanovesicles can release photothermal energy and release drugs depending on the nanovesicle formulation (Carter et al., 2014). Thus, it provides the potentials not only as multimodal photonic contrast agents but also as triggering drug release carriers. In this study, radiolabeling of PLN encapsulating drugs can provide critical *in vivo* quantitative information on these PLN for diagnosing and treating disease.

Liposomes can be used for applications such as drug delivery and imaging due to their size-controllable self-assembly nature (Torchilin, 2005, Malam et al., 2009). Lipid nanovesicles are especially useful platforms due to their high drug loading and manufacturing versatility among current clinical trials' nanoparticles (Torchilin, 2005, Malam et al., 2009, Chang and Yeh, 2012). However, drugs in the liposome can be released at unspecific times due to difficulties in controlling drug encapsulation and drug release. Porphyrin-lipid nanovesicles can be a potential system to overcome this shortcoming by a activatable drug release. *In vivo* tracking of the PLN can get information on the distribution and uptake of the PLN at target sites and its potential efficacy in treatment (Liu et al., 2012). Radiolabeling of liposome nanovesicles with ^{99m}Tc would allow *in vivo* tracking by SPECT (Weers et al., 2009).

So far, radiolabeling of the PLN encapsulating drugs has not been fully studied. Liposome-encapsulated drugs have different biodistributions and toxicities as compared to 'free' drugs (Yan et al., 2008). Thus, in this study we investigated the radiolabeling of a model drug loaded PLN with ^{99m}Tc. Specifically, we evaluated the stability of drug encapsulation and integrity of the ^{99m}Tc-PLN. Radiolabeling of PLN encapsulating drugs can provide *in vivo* quantitative information on PLN for diagnosing and treating diseases. We used ^{99m}Tc surface radiolabeling method due to its mild labeling condition, which can potentially apply for the labeling of the final pharmaceutical product and allow encapsulated drugs to remain inert inside the PLN (Lee et al., 2013b). Stable ^{99m}Tc labeling of PLN is ideal because ^{99m}Tc (physical half life=6h) is inexpensive and readily available. Gamma scintigraphy (SPECT) can be used to evaluate their potential clinical application studies such as lung treatments (Richardson et al., 1979, Weers et al., 2009, Conway, 2012, Elbayoumi and Torchilin, 2006, Phillips, 1999).

In this study, we optimized PLN composition for stable drug encapsulation and ^{99m}Tc labeling parameters to yield a high labeling efficiency without a significant impact on the liposome integrity and drug encapsulation. The ^{99m}Tc-PLN were investigated by size exclusion low pressure liquid chromatography (LPLC) that was recently developed for cholesterol rich liposome analysis (Lee et al., 2013b). With this analytical method, both ^{99m}Tc binding and release from the liposome outer leaflet, model of encapsulated drug leakage, and the detachment of fluorescent lipid can be evaluated simultaneously.

2. Materials and Methods

All chemicals were purchased from Sigma-Aldrich (St. Louis, MO, USA) unless specified otherwise. Pyropheophorbide-a-lipid ($C_{57}H_{79}N_5PO_9$, M.W.=1012.3g/mole) was provided by Lovell's research group (Lovell et al., 2011). All other lipids were purchased from Avanti

Polar Lipids, including dipalmitoylphosphatidyl-choline (DPPC), 1,2-distearoyl-sn-glycero-3-phosphoethanolamine-N-[methoxy (polyethylene glycol)-2000] (DSPE-PEG2000).

2.1. Porphyrin-Lipid Nanoparticle Preparation

Porphyrin-Lipid Nanovesicles were prepared by probe sonication. Briefly, a lipid film (total 5mg per vial) was formed by removing chloroform solvent under nitrogen at room temperature using either porphyrin lipid: cholesterol (CH): PEG=45:50:5 molar ratio or porphyrin lipid: CH =50:50 molar ratio formulation. Residual chloroform was removed by placing the films overnight in a lyophilizer. To encapsulate calcein as a model drug, a lipid film was reconstituted in a self-quenched concentration of calcein (50mM, 1mL). The PLN were eluted through a size-exclusion gel chromatography column (sepharose CL 4B, pre-equilibrated with pH 7.0 saline buffer) to remove free calcein. The presence of PLN in the column fractions was analyzed by the measurement of entrapped calcein.

2.2. Radiolabeling of PLN

The PLN (0.4 mL in 0.9% NaCl) were radiolabeled using sodium pertechnetate $Na^+[^{99m}TcO_4^-]$ as described previously (Farr et al., 1985, Weers et al., 2009, Koizumi et al., 1992). Briefly, 0.2mL of $Na^+[^{99m}TcO_4^-]$ (1 mCi $^{99m}TcO_4^-$/0.08mL 0.9%NaCl) in 1.5% NaCl (Technelite® $^{99}Mo/^{99m}Tc$ generator from Lantheus Medical Imaging, Inc.) was added to a sterile vial containing PLN (0.4 mL at 50mM calcein) and the contents were shaken for approximately 30 sec. A volume of 0.02 mL of 2 mM $SnCl_2$ (Lot No.452335) solution prepared in $SnCl_2$ dissolved in 1mM HCl as a reducing agent for 10 min at 22°C, filtered through a 0.22 μm sterilizing filter (MillexGV filter unit, Millipore, Billerica, MA, USA) was then added into the vial. The vial was gently mixed for approximately 30 sec and incubated at room temperature for 10 min. An aliquot of known volume was withdrawn for determination of the specific activity (mCi/mg) of the radiolabeled PLN. The specific radioactivity concentration was 5.3±0.5mCi/mL (n=3). A further aliquot of known volume was withdrawn to determine the radiochemical purity. The ^{99m}Tc-PLN were assessed to evaluate its radiolabeling efficiency and stability with ITLC and LPLC.

2.3 PLN characterization

PLN's size and size distribution were determined by dynamic light scattering (DLS) measurements using a Malvern instrument (NANO ZS, Malvern Instruments, CA, USA). The Z-average particle size was measured in triplicate. The integrity of the radiolabeled PLN was determined by several analytical methods. The samples were assessed by size exclusion LPLC equipped with a size exclusion Sepharose CL 6B column (25 × 300 mm, GE healthcare, 1.5% NaCl, pH 6.8;0.8mL/min)(modified for pressure pump use), an UV monitor, a fluorescent monitor and an on-line flow radioactivity detector (Bioscan Inc., Washington, DC, USA)(Lee et al., 2013b). The radiochemical purity of ^{99m}Tc-PLN was also evaluated by ascending ITLC (Gelman Sciences, Inc., Ann Arbor, MI, USA) using 100% acetone as the solvent phase (Arulsudar et al., 2003). Calcein entrapment efficiency was determined by fluorescent intensity change at 495nm Excitation (Ex)/ 515nm Emission (Em), using a fluorescence microplate reader (SpectraMax M2, Molecular Devices) after adding the detergent Triton X 100 (TX100, 0.02% final concentration). The drug

encapsulation efficiency was calculated using the following formula: F_t/F_0 where F_t is the fully dequenched drug fluorescence intensity after the addition of TX100 and F_0 is the fluorescence intensity of drug before the addition of TX100.

3. Results and discussion

3.1. PLN formation

In this study we used cholesterol rich formulation (Porphyrin lipid: Cholesterol (CH): PEG=45:50:5 or Porphyrin lipid: CH =50:50)) (For all the presented data except a long term drug encapsulation study, Porphyrin lipid: Cholesterol (CH): PEG=45:50:5 formulation was used due to its stable formulation *in vivo*). LPLC analysis was performed to test the stability of the PLN and drug encapsulation. The elution results of PLN encapsulating calcein demonstrated the clear separation of free calcein from the calcein encapsulated PLN (Figure 1a). PLN with cholesterol rich composition that was eluted through a size-exclusion gel chromatography column (sepharose CL 4B) showed a dark green color and was collected in the early stage successfully. The particle size and size distribution of PLN were analyzed with dynamic light scattering. The size was determined to be 141.6±1.9 nm (P.I. <0.16) after the LPLC size exclusion column (before size exclusion column 134.4±1.8 nm (P.I.<0.29), which indicates nano-size PLN formations (Figure 1b)(For Porphyrin lipid: CH =50:50, the size was 96.9± 0.3 nm (P.I.<0.20) before size exclusion column). The characteristic UV-Vis peak of PLN due to its porphyrin structure was also analyzed before and after ^{99m}Tc radiolabeling. UV/Vis spectra of the PLN indicate that the porphyrin's structure of the PLN remained inert in the nanoparticles (note that the ^{99m}Tc labeled PLN have the same spectrum) (Figure 1c). The LPLC method was used to analyze cholesterol rich PLN, which is an optimal analytical tool for PLN of this size range. The LPLC results showed that the liposomal peaks were detected by a UV/Vis monitor set at 485 nm and 680 nm, also by fluorescent monitor set at 420nm Ex/ 680nm Em. At 485nm, strong calcein and porphyrin absorbance could be detected at the same time. At 680nm, only strong porphyrin absorbance could be detected. At 420nm Ex/ 680nm Em, only strong porphyrin fluorescence could be detected. Interestingly, all three peaks overlapped each other, and all the peaks were different from free calcein (Figure 2 and see also supporting information Figure S1). That indicates calcein had been successfully encapsulated. To check liposome integrity, the stability test by Triton X 100, known as a liposome destabilizing surfactant, was performed. After Triton X 100 addition to the PLN solution (10uL:100uL) the LPLC analysis showed that the PLN were destabilized. The fluorescent detection of free calcein at 485nm Ex/ 515nm Em clearly demonstrated calcein encapsulation (Supporting Information Figure S1). The drug encapsulation was also evaluated by a 96 well fluorescent reader. Upon the addition of Triton X 100, the fluorescent signal increased rapidly (Figure 3). These LPLC and fluorescence microplate reader's data strongly support that calcein was stably encapsulated by the PLN.

We also studied long-term drug leakage rates of PLN by the fraction of drug release as a function of time, R(x),

$$R(x)=1-(\frac{F_x(final)-F_x(initial)}{F_0(final)-F_0(initial)}.\frac{F_0(final)}{F_x(final)})$$

where x is day, and F(initial) and F(final) are the fluorescence intensity before and after adding the Triton X-100(Wang et al., 2006) (Figure 4). Lower R(x) value indicated that encapsulated drug did not leak out for a longer time, suggesting that cholesterol-rich PLN are a stable liposome nanoparticle. These results demonstrated that PLN have along term stability like CTAT/SDBS equilibrium vesicles. Porphyrin lipid has only one hydrophobic tail. The addition of cholesterol increases the hydrophobic volume and critical packing parameter of PLN. As a result, the cholesterol formulation improves thermo-dynamical liposome stability of the PLN.

3.2. Radiolabeling chemistry and analysis of PLN

The ^{99m}Tc labeling of PLN was efficient in the presence of stannous chloride (80 μM) in 0.91mM ascorbic acid or 1mM HCl, producing ^{99m}Tc-PLN with a high labeling yield: 96.1± 2.8% (n=3) and 88.2±3.4% (n=3), when determined by ITLC and LPLC, respectively. The LPLC profiles traced by UV, Fluorescence, and online radioactivity monitor indicate that the ^{99m}Tc-radiolabeled PLN had a mono-disperse peak (between 10 and 20min) at the same elution time of control PLN (Figure 5). The peak shape and retention time of these peaks were identical to those of the original unlabeled PLN, indicating that the ^{99m}Tc labeling condition did not change the size of PLN. This LPLC analysis also demonstrated that the integrity of PLN was maintained during ^{99m}Tc radiolabeling process. This finding indicates that encapsulated calcein remained inert inside the liposome and the PLN structure was not disrupted by the ^{99m}Tc labeling condition or the LPLC elution process. Of note, the LPLC retention time of ^{99m}Tc pertechnetate was about 45 min (Lee et al., 2013a). This LPLC system equipped with multi-signal detectors has been shown in this study as a very useful analysis for the determination of liposome integrity and drug encapsulation.

After radiolabeling, the drug encapsulation was evaluated by a 96 well fluorescent reader. Triton X 100 was added to ^{99m}Tc-PLN solution after 3 weeks storage at 4°C (Figure 6). The fluorescent intensity at 485nm Ex/ 515nm Em indicates that the encapsulated calcein remained inert in the PLN. The result suggests that ^{99m}Tc labeling did not affect the drug encapsulation of PLN. The ^{99m}Tc binding stability was also evaluated after 24h storage at 4°C (Figure 7). The elution peak of ^{99m}Tc-PLN after 24h storage at 4°C was the same as that of ^{99m}Tc-PLN immediately after radiolabeling, indicating that the ^{99m}Tc binding to PLN was very stable. The elution peak of ^{99m}Tc pertechnetate was observed in the later elution time (about 45–50 min) (less than 20%). The ^{99m}Tc binding stability against Triton X 100 was also evaluated after 24h storage at 4°C(Figure 8). The elution peak of ^{99m}Tc pertechnetate was observed (about 40%). Interestingly, calcein leakage (less than 10%) was not greater than that from the control PLN (about 30%) after Triton X 100 treatment. The main monodisperse peak of ^{99m}Tc-PLN was still observed. Considering that the addition of Triton X 100 into the PLN solution can induce calcein leakage according to the fluorescent study (Figure 6), it suggests that Triton X 100 makes the PLN leaky while leaving their size unaltered at the condition of Triton X 100 to PLN solution =10 μL:100 μL. The size

measurement of the PLN after adding Triton Xby DLS confirmed this suggestion. However, it cannot be excluded the possibility of the further micellization by adding more Triton X 100.

There are two potential binding sites of ^{99m}Tc to the PLN surface after reducing the oxidation state of $^{99m}Tc^{+7}$ to $^{99m}Tc^{+4}$: one possible site is complexation with the phosphate moieties on the surface of the PLN(Phillips, 1999, Lee et al., 2013b), and the second site is that $^{99m}Tc^{+4}$ can possibly bind to aporphyrin functional group (Spagnul et al., 2013)(see Supporting Information Figure S2). These two potential binding sites of PLN may provide radiolabeling by two different radionuclides. In addition, negatively charged calcein can interact with positively charged ^{99m}Tc *via* an electrostatic interaction if calcein leaks out. Of note, the radiolabeling of ^{99m}Tc to PLN appeared to be formulation dependent. With PEG formulation for the PLN, a poor labeling yield (less than <40%) was detected in the presence of stannous chloride in 0.91mM ascorbic acid. The reason is not clear currently. ILTC analysis using acetone as the solvent also demonstrated successful radiolabeling of ^{99m}Tc-PLN. With acetone as the solvent, ^{99m}Tc-PLN remained at the origin and $^{99m}TcO_4^-$ eluted along with the solvent to the solvent front.

4. Conclusions

The ^{99m}Tc labeling of PLN with stannous chloride as a reducing agent in HCl produced ^{99m}Tc-PLN with high radiochemical and drug encapsulation stability, while maintaining the liposome integrity. This was confirmed by ITLC and a LPLC system equipped with multi-detectors. This study confirmed that the encapsulated calcein did not alter the stability of PLN and ^{99m}Tc labeling, and ^{99m}Tc labeling did not change the calcein encapsulation properties of PLN. Thus, ^{99m}Tc- PLN will be able to be used for tracking the *in vivo* biodistribution of PLN by SPECT imaging.

Supplementary Material

Refer to Web version on PubMed Central for supplementary material.

Acknowledgments

This research was supported by the intramural research program of Clinical Center, NIH.

References

Arulsudar N, Subramanian N, Mishra P, Sharma RK, Murthy RS. Preparation, characterisation and biodistribution of 99mTc-labeled liposome encapsulated cyclosporine. J Drug Target. 2003; 11:187–96. [PubMed: 13129826]

Carter KA, Shao S, Hoopes MI, Luo D, Ahsan B, Grigoryants VM, Song W, Huang H, Zhang G, Pandey RK, Geng J, Pfeifer BA, Scholes CP, Ortega J, Karttunen M, Lovell JF. Porphyrin-phospholipid liposomes permeabilized by near-infrared light. Nature Communications. 2014; 5:3546.

Chang HI, Yeh MK. Clinical development of liposome-based drugs: formulation, characterization, and therapeutic efficacy. International journal of nanomedicine. 2012; 7:49–60. [PubMed: 22275822]

Conway J. Lung imaging - Two dimensional gamma scintigraphy, SPECT, CT and PET. Advanced Drug Delivery Reviews. 2012; 64:357–68. [PubMed: 22310158]

Elbayoumi TA, Torchilin VP. Enhanced accumulation of long-circulating liposomes modified with the nucleosome-specific monoclonal antibody 2C5 in various tumours in mice: gamma-imaging studies. European Journal of Nuclear Medicine and Molecular Imaging. 2006; 33:1196–205. [PubMed: 16763815]

Ellis GA, Mcgrath NA, Palte MJ, Raines RT. Ribonuclease-Activated Cancer Prodrug. ACS medicinal chemistry letters. 2012; 3:268–72. [PubMed: 22611478]

Farr SJ, Kellaway IW, Parryjones DR, Woolfrey SG. TECHNETIUM-99M AS A MARKER OF LIPOSOMAL DEPOSITION AND CLEARANCE IN THE HUMAN-LUNG. International journal of pharmaceutics. 1985; 26:303–16.

Goga L, Pushpakumar SB, Perez-Abadia G, Olson P, Anderson G, Soni CV, Barker JH, Maldonado C. A novel liposome-based therapy to reduce complement-mediated injury in revascularized tissues. J Surg Res. 2011; 165:e51–7. [PubMed: 21074780]

Guo C, Wu X, Yan M, Dong Q, Yin S, Sato T, Liu S. The visible-light driven photocatalytic destruction of NO(x) using mesoporous TiO2 spheres synthesized via a “water-controlled release process”. Nanoscale. 2013; 5:8184–91. [PubMed: 23893071]

Jin CS, Lovell JF, Chen J, Zheng G. Ablation of hypoxic tumors with dose-equivalent photothermal, but not photodynamic, therapy using a nanostructured porphyrin assembly. ACS nano. 2013; 7:2541–50. [PubMed: 23394589]

Koizumi K, Uchiyama G, Arai T, Ainoda T, Yoda Y. A new liver functional study using Tc-99m DTPA-galactosyl human serum albumin: evaluation of the validity of several functional parameters. Ann Nucl Med. 1992; 6:83–7. [PubMed: 1320389]

Lee J, Park J, Singha K, Kim WJ. Mesoporous silica nanoparticle facilitated drug release through cascade photosensitizer activation and cleavage of singlet oxygen sensitive linker. Chem Commun (Camb). 2013a; 49:1545–7. [PubMed: 23325385]

Lee JH, Cheng KT, Malinin V, Li Z, Yao Z, Lee SJ, Gould CM, Olivier KN, Chen C, Perkins WR, Paik CH. (99m)Tc-labeled therapeutic inhaled amikacin loaded liposomes. Journal of liposome research. 2013b; 23:336–42. [PubMed: 23879241]

Liu TW, Macdonald TD, Shi J, Wilson BC, Zheng G. Intrinsically copper-64-labeled organic nanoparticles as radiotracers. Angew Chem Int Ed Engl. 2012; 51:13128–31. [PubMed: 23154923]

Lovell JF, Jin CS, Huynh E, Jin H, Kim C, Rubinstein JL, Chan WC, Cao W, Wang LV, Zheng G. Porphysome nanovesicles generated by porphyrin bilayers for use as multimodal biophotonic contrast agents. Nature materials. 2011; 10:324–32. [PubMed: 21423187]

Malam Y, Loizidou M, Seifalian AM. Liposomes and nanoparticles: nanosized vehicles for drug delivery in cancer. Trends Pharmacol Sci. 2009; 30:592–9. [PubMed: 19837467]

Ng KK, Lovell JF, Vedadi A, Hajian T, Zheng G. Self-assembled porphyrin nanodiscs with structure-dependent activation for phototherapy and photodiagnostic applications. ACS nano. 2013; 7:3484–90. [PubMed: 23464857]

Phillips WT. Delivery of gamma-imaging agents by liposomes. Advanced Drug Delivery Reviews. 1999; 37:13–32. [PubMed: 10837724]

Richardson VJ, Ryman BE, Jewkes RF, Jeyasingh K, Tattersall MN, Newlands ES, Kaye SB. Tissue distribution and tumour localization of 99m-technetium-labelled liposomes in cancer patients. Br J Cancer. 1979; 40:35–43. [PubMed: 475960]

Snyder JW, Greco WR, Bellnier DA, Vaughan L, Henderson BW. Photodynamic therapy: a means to enhanced drug delivery to tumors. Cancer research. 2003; 63:8126–31. [PubMed: 14678965]

Spagnul C, Alberto R, Gasser G, Ferrari S, Pierroz V, Bergamo A, Gianferrara T, Alessio E. Novel water-soluble Tc-99m(I)/Re(I)-porphyrin conjugates as potential multimodal agents for molecular imaging. J Inorg Biochem. 2013; 122:57–65. [PubMed: 23474539]

Torchilin VP. Recent advances with liposomes as pharmaceutical carriers. Nature Reviews Drug Discovery. 2005; 4:145–60. [PubMed: 15688077]

Wang X, Danoff EJ, Sinkov NA, Lee JH, Raghavan SR, English DS. Highly efficient capture and long-term encapsulation of dye by catanionic surfactant vesicles. Langmuir : the ACS journal of surfaces and colloids. 2006; 22:6461–4. [PubMed: 16830982]

Weers J, Metzheiser B, Taylor G, Warren S, Meers P, Perkins WR. A gamma scintigraphy study to investigate lung deposition and clearance of inhaled amikacin-loaded liposomes in healthy male volunteers. J Aerosol Med Pulm Drug Deliv. 2009; 22:131–8. [PubMed: 19422313]

Yan H, Cheng C, Haouala A, Krueger T, Ballini JP, Peters S, Decosterd LA, Letovanec I, Ris HB, Andrejevic-Blant S. Distribution of free and liposomal doxorubicin after isolated lung perfusion in a sarcoma model. The Annals of thoracic surgery. 2008; 85:1225–32. [PubMed: 18355500]

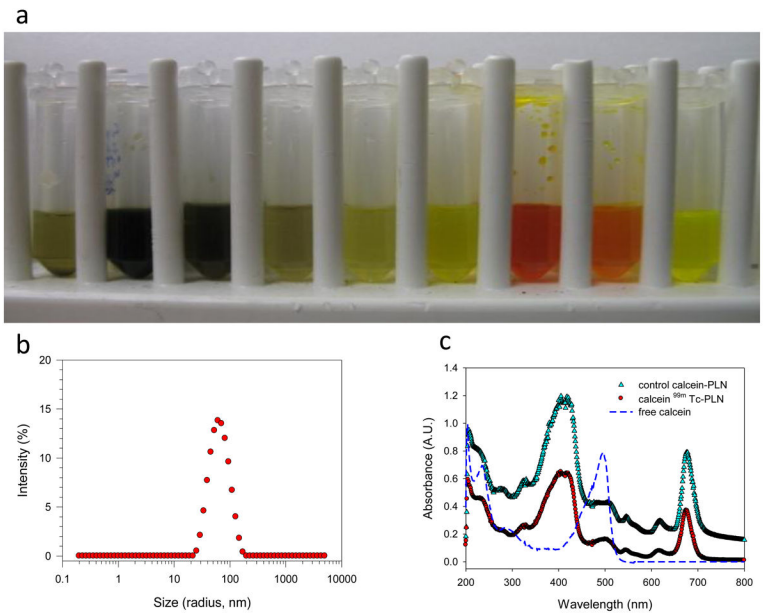

Figure 1.

Analysis results of PLN encapsulating drug (i.e., calcein as a model drug): a) collection vials from a size-exclusion gel chromatography column (from left to right collected, flow rate 0.25 mL/min), demonstrating that calcein encapsulated in PLN was well separated from free calcein (0.5 mL of 7,8, and 9 samples from 5 mL sample solution were transferred to demonstrate the effects); b) particle size analysis by DLS, showing a monodisperse particle size distribution; and c) UV/Vis spectra of PLN encapsulating calcein and ^{99m}Tc-PLN that are different from free calcein.

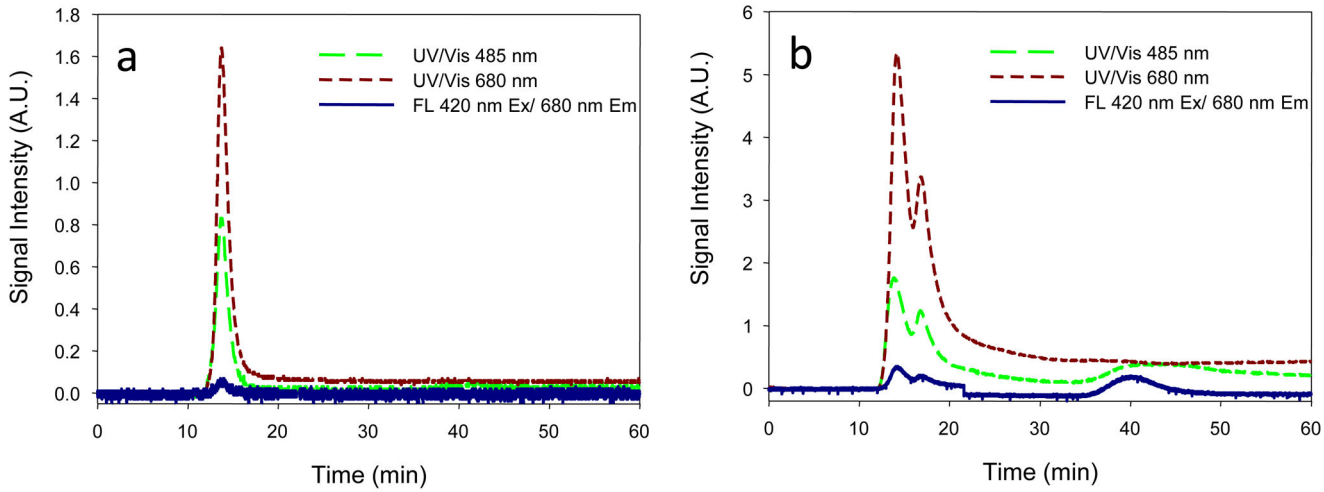

Figure 2.

LPLC Analysis results of PLN encapsulating drug before and after Triton X 100 addition: (a) PLN before adding Triton X 100; (b) PLN after adding Triton X 100, demonstrating mono-disperse PLN, the integrity of PLN, calcein encapsulation detected by multi-detectors.

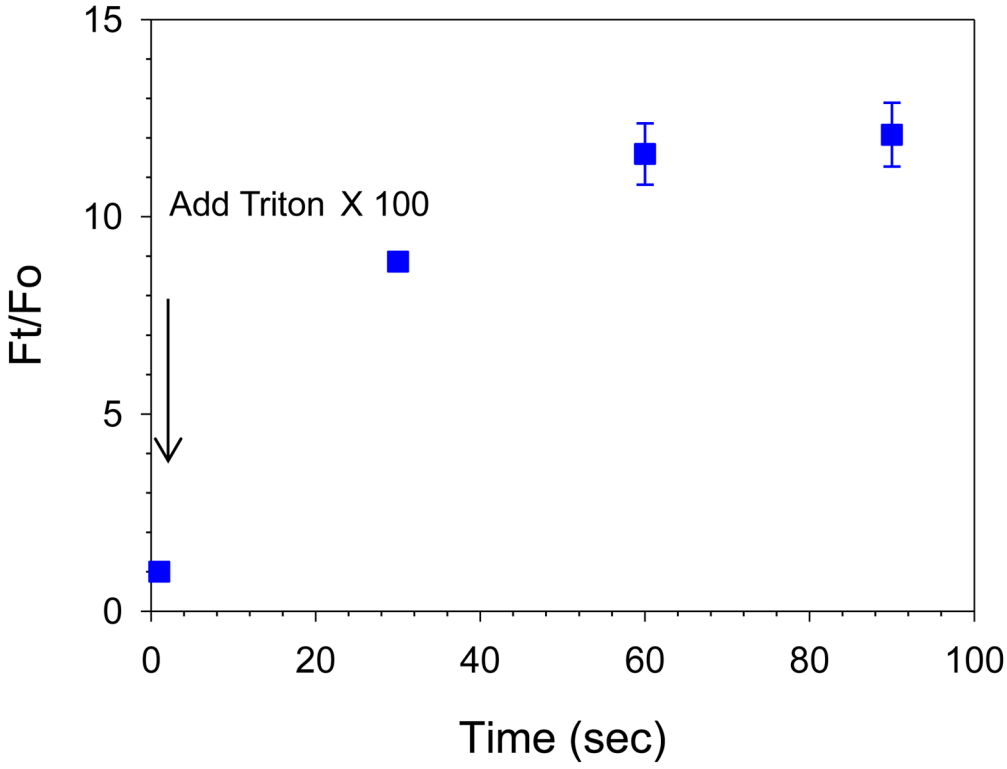

Figure 3.

Drug encapsulation analysis of PLN by a 96 well fluorescence microplate. After the addition of Triton X 100 the fluorescent intensity was monitored at different time. The dequenched fluorescent signal after adding Triton X 100 due to released calcein from PLN contributed to the increased fluorescent signal, demonstrating successful drug encapsulation.

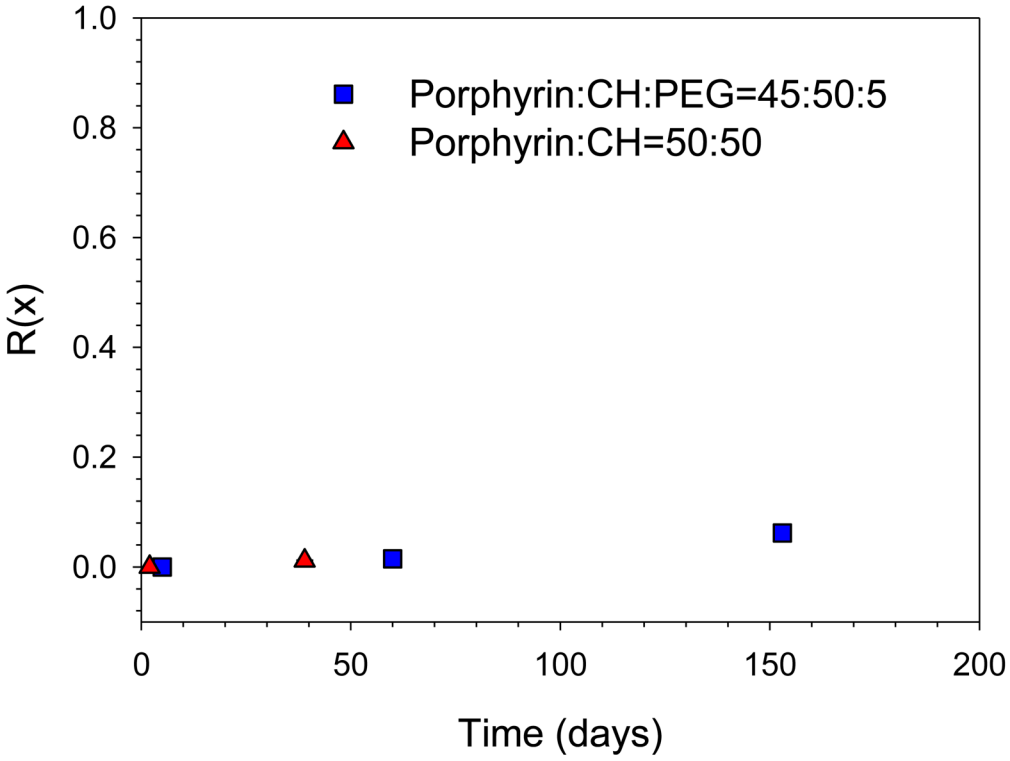

Figure 4.

A long term drug encapsulation of PLN using by the fraction of drug release as a function of time. Lower R(x) value indicated that encapsulated drug did not leak out for a longer time, suggesting that cholesterol-rich PLN is a stable liposome nanoparticle.

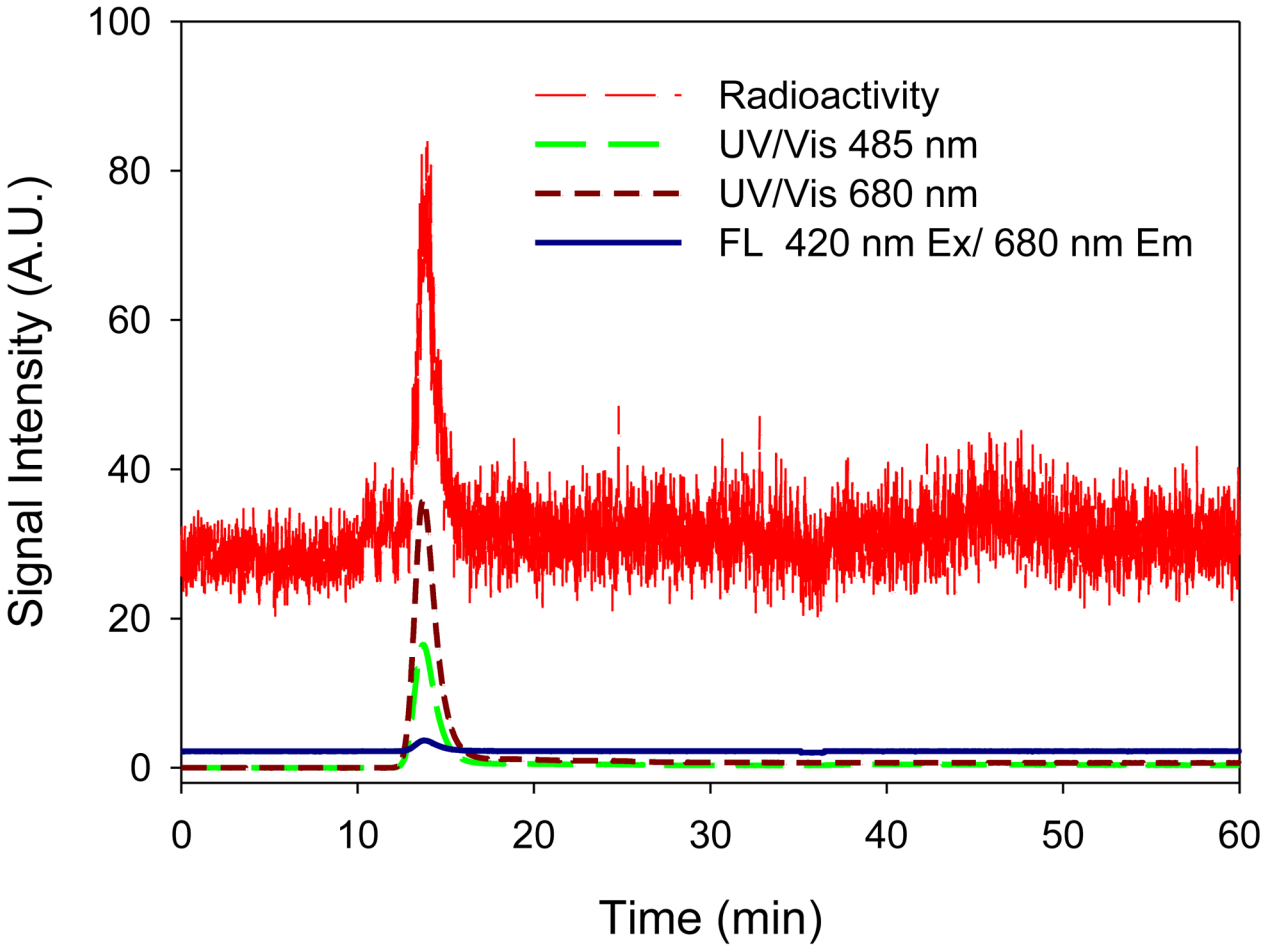

Figure 5.

The LPLC analysis of ^{99m}Tc-radiolabeled PLN. ^{99m}Tc-PLN demonstrated a monodisperse elution peak and no drug leakage, showing ^{99m}Tc binding to PLN, the integrity of ^{99m}Tc-PLN, and the drug encapsulation maintenance detection traced by UV, Fluorescence, and online radioactivity monitors.

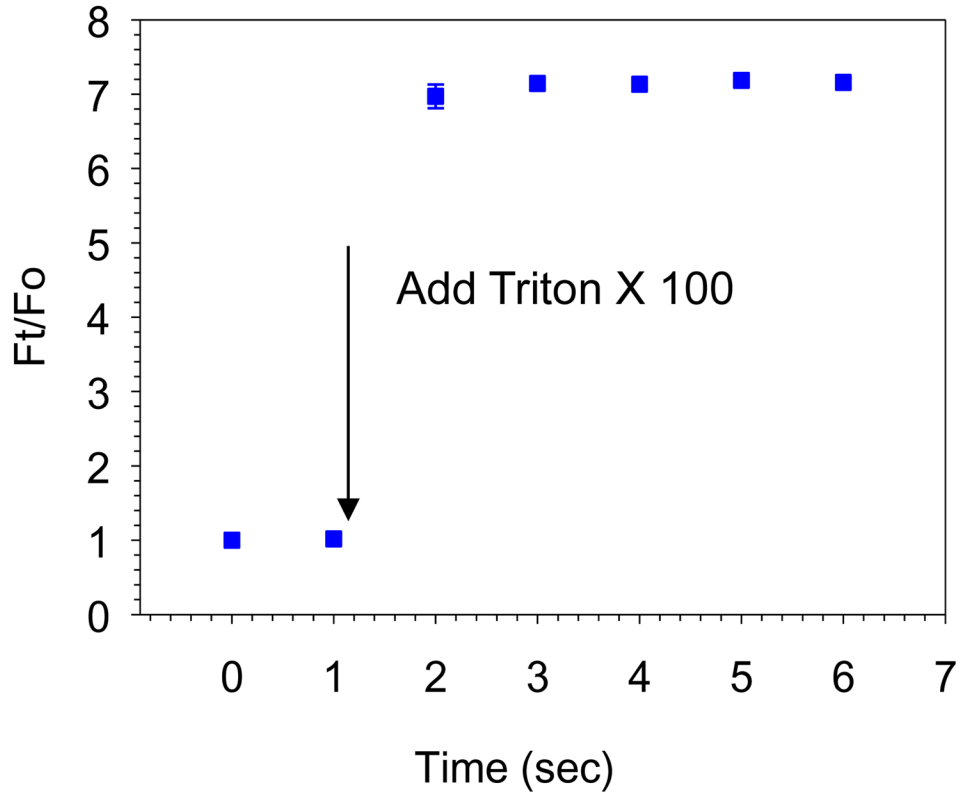

Figure 6.

Drug encapsulation analysis of ^{99m}Tc-radiolabeled PLN by a 96 well fluorescence microplate. After the addition of Triton X 100 the fluorescent intensity increase was monitored, demonstrating that the drug encapsulation remained inert.

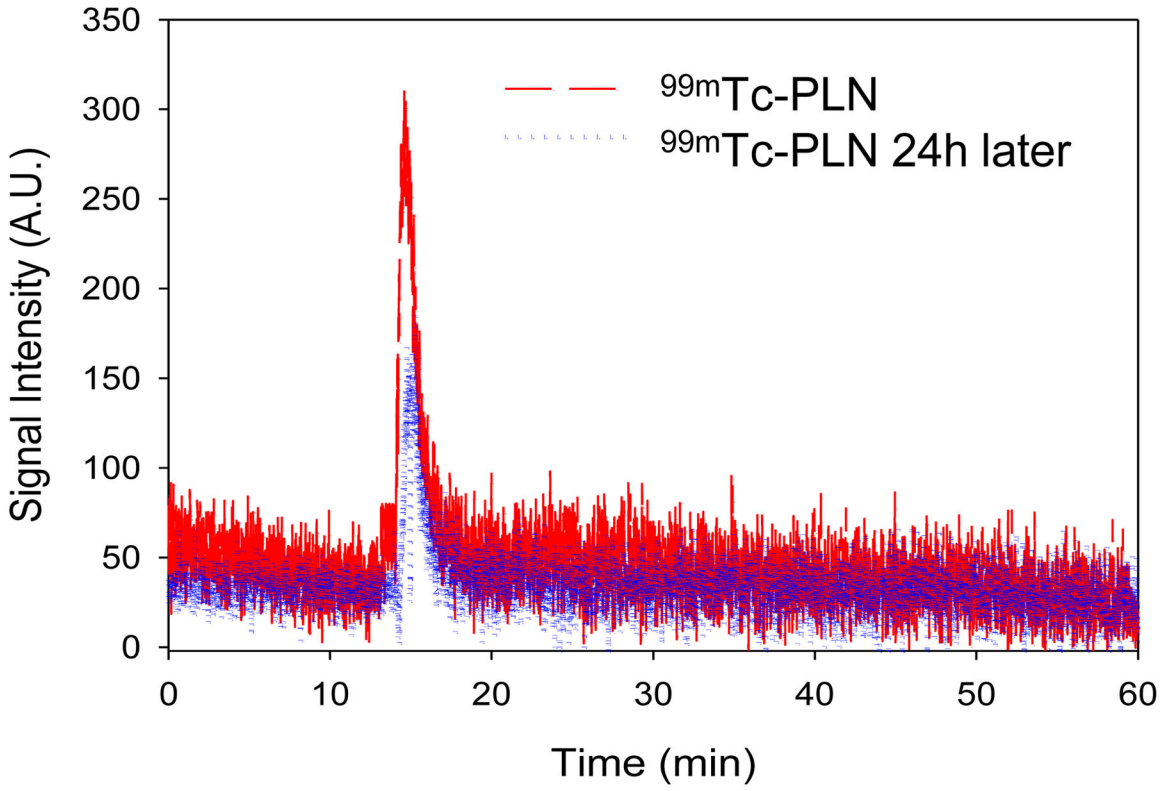

Figure 7.
^{99m}Tc binding stability after 24 h storage at 4°C. Two peaks of ^{99m}Tc-PLN were overlapped each other, showing the ^{99m}Tc binding to PLN was very stable

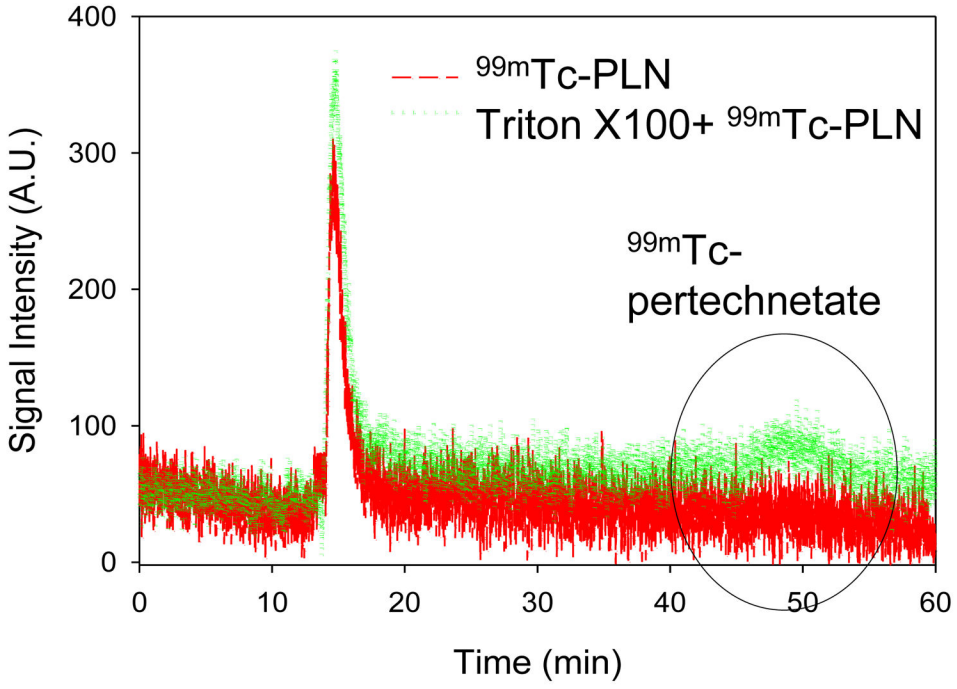

Figure 8.

^{99m}Tc binding stability of ^{99m}Tc-PLN against Triton X 100 addition after 24 h storage at 4°C. About 40% ^{99m}Tc detachment was observed and the main monodisperse peak of ^{99m}Tc-PLN remained inert.